

# KINETIC THEORY OF ELECTRON-PLASMA AND ION-ACOUSTIC WAVES IN NONUNIFORMLY HEATED LASER PLASMAS

*B. B. Afeyan\**

*R. P. J. Town††*

*A. E. Chou†*

*W. L. Kruer*

*J. P. Matt\*\**

## Introduction

When a high-intensity laser illuminates a plasma, large-scale nonuniformities in the laser spatial profile will cause differential heating in the plasma giving rise to steep temperature gradients, nonlocal heat transport, heat flux inhibition,<sup>1</sup> and non-Maxwellian inverse bremsstrahlung heating especially in laser hot spots.<sup>2,3</sup> Laser-spatial-profile nonuniformities can contribute to the dephasing of three-wave-parametric instabilities in the usual way.<sup>4</sup> However, the effect of these nonuniformities on the *background plasma* and kinetic characteristics of waves, which then affect instabilities in a fundamental way, has in the past been largely ignored.<sup>5</sup> We begin to address that in this article by examining the behavior of plasma waves using velocity distribution functions (VDFs) obtained from Fokker–Planck (FP) simulations of nonuniformly heated, large-scale plasmas. Laser speckle patterns are taken into account, the resulting nonuniform heating is simulated, and their consequences on electron-plasma wave (EPW) and ion-acoustic wave (IAW) properties are calculated by solving the appropriate kinetic dispersion relations. Significant changes in the properties of these waves are uncovered that shed light on some key puzzles in recent laser–plasma interaction experiments. One concerns the stimulated Raman scattering instability (SRS), which involves light scattering off EPWs.<sup>6</sup> SRS is observed from densities that are too low where the VDFs to have been Maxwellian at the measured temperature.<sup>7</sup> Similarly, instabilities involving ion waves<sup>8</sup> seem to be suppressed at high densities in the strong ion-wave damping limit, and stimulated Brillouin scattering (SBS) is observed to be anticorrelated with SRS.<sup>9</sup> In addition, high-Z plasmas have been observed to exhibit SRS levels

that depend strongly on ion wave characteristics.<sup>10</sup> In those experiments, the potential for Langmuir decay instability (LDI) to saturate SRS was brought into question and resolved by invoking reduced damping rates of EPWs via the mechanism discussed in this article.<sup>10,5</sup> Moreover, crossed beam SRS and SRS gains have been shown to be anomalously low with randomly displaced frequency peaks.<sup>11</sup> We will show that this is to be expected whenever the instabilities occur in laser hot spots where the frequencies and damping rates of the waves are modified due to non-Maxwellian VDF effects.

## Description of Simulations

The use of random phase plates (RPPs) was pioneered over a decade ago in laser–plasma interaction experiments,<sup>12</sup> and they have been used ever since. RPPs are meant to replace unpredictable and unwarranted large-scale variations in laser intensity with a statistically well defined spiky interference or speckle pattern.<sup>13</sup> Given any such nonuniform laser illumination profile, it is important to obtain the resulting electron VDFs from an FP calculation as the plasma is heated to inertial confinement fusion (ICF) relevant temperatures of 2 or 3 keV. We have done this with both the FPI<sup>3</sup> and SPARK<sup>14</sup> codes in large 1D simulations and smaller 2D boxes for comparison. We will concentrate on the set of comprehensive 1D runs using FPI in this article and report on 2D results elsewhere. These simulations used a lateral cut across a 0.35- $\mu\text{m}$ -wavelength RPP beam, which was 211- $\mu\text{m}$  wide. The plasma had two side (or “moat”) regions of the same width as the beam, all held at a density of tenth critical. The ionization states were low to moderate ( $\bar{Z} = \langle Z^2 \rangle / \langle Z \rangle = 5, 10, 20$ ). The angular dependence of the VDF is expanded in Legendre polynomials in FPI up to order 3. Inspection of the values showed that the  $|f_2|/f_0$  ratio was below 1 in all regions where  $f_0$  was not vanishingly small. Only  $f_0$  is used in the present

\*University of California, Davis–Livermore, Livermore, CA

†University of California, Los Angeles, Los Angeles, CA

\*\*INRS Energie-Materiaux, Varennes, Quebec, Canada

††LLE, University of Rochester, Rochester, NY

analysis. Beyond each edge of the 211- $\mu\text{m}$ -wide beam, the intensity was allowed to fall off linearly over 73  $\mu\text{m}$ , and then there was a 139- $\mu\text{m}$  unheated region before reaching the simulation box boundaries which were maintained at the initial temperature of 300 eV. These large, unheated regions essentially eliminate the effects of boundaries on the transport physics within the beam because hot electrons generated in hot spots are quickly transported into the large cooler regions surrounding the beam before being absorbed at the boundaries and reemitted with an equivalent flux at the prescribed wall temperature.

## Simulation Results and Interpretation

To show the resulting VDFs, we resort to the shorthand of a set of super-Gaussian functions, which were first introduced by Dum in a number of different plasma physics contexts,<sup>15</sup> and that were found to be ideal for the description of quasi-steady-state, uniform-intensity-illumination, laser-plasma-heating, and transport simulations by Matte using his FPI code.<sup>2,3</sup> These Dum–Langdon–Matte (DLM) VDFs may be written in the form

$$f_e = C(n) \frac{N_{e0}}{v_e^3} \exp\left(-\left(\frac{|v|}{\alpha_e v_e}\right)^n\right) \quad (1)$$

where  $v_e^2 = T_e/m_e$  and the constant

$$\alpha_e = \left(\frac{3\Gamma(3/n)}{\Gamma(5/n)}\right)^{1/2} \quad (2)$$

is chosen to ensure the proper definition of temperature in terms of the second moment of the 3D distribution function:

$$\langle v^2 \rangle = 3v_{th}^2. \quad (3)$$

The normalization prefactor is

$$C(n) = \left(\frac{1}{4\pi\alpha_e^3}\right) \left(\frac{n}{\Gamma(3/n)}\right), \quad (4)$$

which ensures that the zeroth moment of the 3D distribution function is the density  $N_{e0}$ . In the standard theory of non-Maxwellian inverse bremsstrahlung heating,<sup>2,3</sup> as the laser intensity is increased, the exponent  $n$  increases from the Maxwellian limit of  $n = 2$  to the limit where electron–electron collisions are entirely negligible,  $n = 5$ . These distribution functions will

have increasingly more flattened cores and depleted tails. For uniform laser illumination cases, Matte<sup>3</sup> has obtained the connection between the exponent  $n$  and parameters that characterize the laser–plasma system. With the laser intensity  $I$  defined in units of  $10^{15} \text{ W/cm}^2$ , laser wavelength  $\lambda_0$  in units of 0.35  $\mu\text{m}$ , and the electron temperature  $T_e$  in keV, the conversion is

$$\begin{aligned} \bar{Z} I_{15, \text{W/cm}^2} \lambda_0^2 \cdot 0.35 \mu\text{m} / T_{e, \text{keV}} \\ = 44.29[(n-2)/(5-n)]^{1.381}. \end{aligned} \quad (5)$$

Because this result neglects the nonlocal heat transport that accompanies spatially nonuniform non-Maxwellian inverse bremsstrahlung heating, we would expect the Matte formula to slightly overestimate the proper DLM exponent  $n$  at the very centers of the hot spots and to severely underestimate the non-Maxwellianity everywhere else in the illuminated region. New FP simulations using RPP beam patterns were performed precisely to overcome these limitations, which a direct reliance on DLMs and the Matte formula would cause.<sup>16,5</sup> The resulting inferred DLM exponents  $n$  from the Ca simulations and those predicted by Matte’s formula are shown in Figure 1 together with the laser intensity distribution and the FP-simulation-obtained temperature profile normalized to the average temperature in the illuminated region. Figure 2 shows the damping rate of EPWs in plasmas, whose  $e^-$  VDFs are given by the FP codes

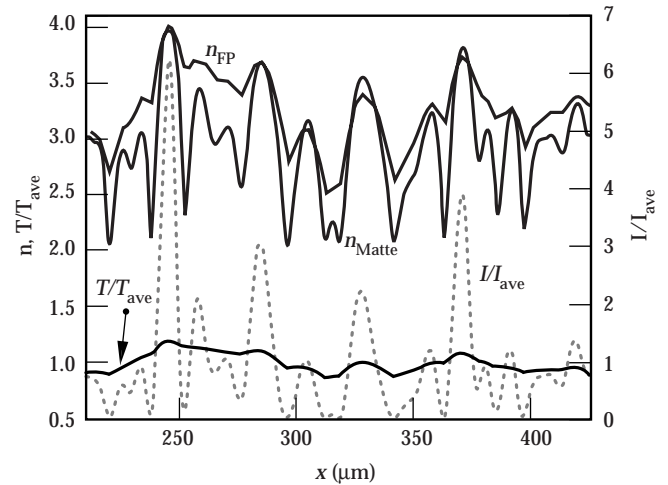


FIGURE 1. The DLM exponent  $n$  and the temperature (normalized to the average temperature in the illuminated region,  $T_{ave} = 2.26 \text{ keV}$ ) extracted from FPI simulations of a Ca plasma at a tenth critical density vs lateral position  $x$  in an  $I/4$  RPP laser beam whose intensity distribution is plotted as  $I/I_{ave}$ , where  $I_{ave} = 2 \times 10^{15} \text{ W/cm}^2$ . Also shown are DLM exponents inferred from the Matte formula, which underestimates the degree of non-Maxwellianity everywhere except at the centers of the hot spots. (50-00-0698-1408pb01)

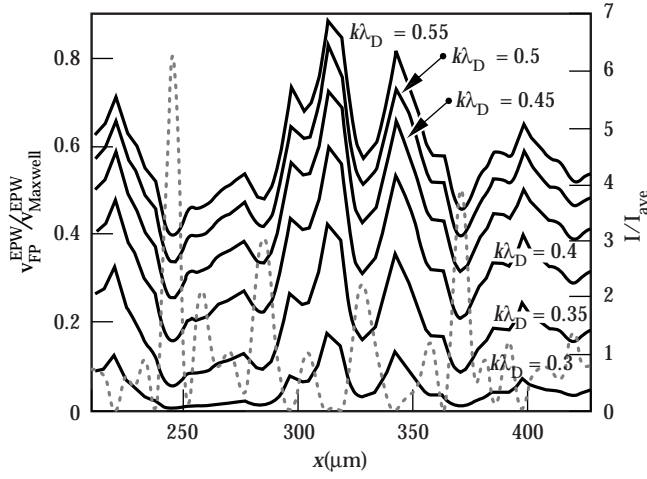


FIGURE 2. EPW damping rates which are solutions of the kinetic dispersion relation using the distribution function obtained from Fokker-Planck simulations, normalized to Maxwellian plasma damping rates at the same average temperature vs lateral position  $x$  for  $k\lambda_{De} = 0.35 - 0.55$ , in steps of 0.05. (50-00-0698-1409pb01)

directly, normalized to that of EPWs in a Maxwellian plasma at the same density and at the same average temperature (inside the illuminated region). The electron susceptibility is given by<sup>6</sup>

$$\chi_e = \frac{\omega_{pe}^2}{N_{e0} k^2 \bar{f}_e} \int \frac{\mathbf{k} \cdot \partial \bar{f}_e / \partial \mathbf{v}}{\omega - \mathbf{k} \cdot \mathbf{v}} d\mathbf{v} \quad (6)$$

$$= \frac{1}{A} \frac{1}{k^2 \lambda_{De}^2} [1 + \zeta_0 I(\zeta_0)] , \quad (7)$$

where

$$\zeta_0 = \left( \omega / \omega_{pe} \right) / (k \lambda_{De}) , \quad (8)$$

$$A = N_{e0} / (2\pi \bar{f}_e) . \quad (9)$$

$N_{e0}$  is the 3D average of the  $e^-$  VDF, and  $\bar{f}_e$  is its 1D average. The Hilbert transform of the normalized VDF is defined via the integral

$$I(\zeta_0) = \int \frac{d\zeta \bar{f}_e(\zeta)}{(\zeta - \zeta_0) \bar{f}_e} . \quad (10)$$

Solving  $1 + \chi_e = 0$  gives us the complex frequencies of EPWs. The resulting damping rates for a Ca plasma at an average temperature of 2.26 keV are shown in Figure 2. Note the order of magnitude reduction in EPW damping rates compared to those in a Maxwellian plasma at the values of  $k\lambda_{De} \approx 0.35$  that typically arise in experiments.

## The Effects of Modified Distribution Functions on IAWs and SBS

The impact of non-Maxwellian  $e^-$  VDFs on IAWs can be seen by noting the factor  $A$  which renormalizes  $k^2 \lambda_{De}^2$  in Eq. (7). It boosts the effective electron temperature that enters the definition of the frequency of an IAW:  $\omega_{IAW}^2 = A c_s^2 k^2$ . The reduced number of slow electrons available to shield the ions causes this IAW frequency increase over that of a Maxwellian plasma. For DLMs, we have calculated this boosting factor analytically to be

$$A(n) = \frac{3[\Gamma(3/n)]^2}{\Gamma(1/n)\Gamma(5/n)} . \quad (11)$$

In Figure 3 we plot the actual  $A$  factor calculated using the VDFs obtained from the FP simulations multiplied by the ratio of the spatially varying temperature, obtained from the FP runs, divided by the average temperature vs lateral position inside the RPP beam for CH, Ne, and Ca plasmas at one-tenth critical density and an average laser intensity of  $2 \times 10^{15} \text{ W/cm}^2$ . RMS fluctuations exceeding 20% are obtained via this ion-acoustic frequency spatial modulation effect due to spatially nonuniform and non-Maxwellian inverse bremsstrahlung heating. Such modulations can help explain the recent crossed beam SBS results of Kirkwood et al.,<sup>11</sup> where anomalously low

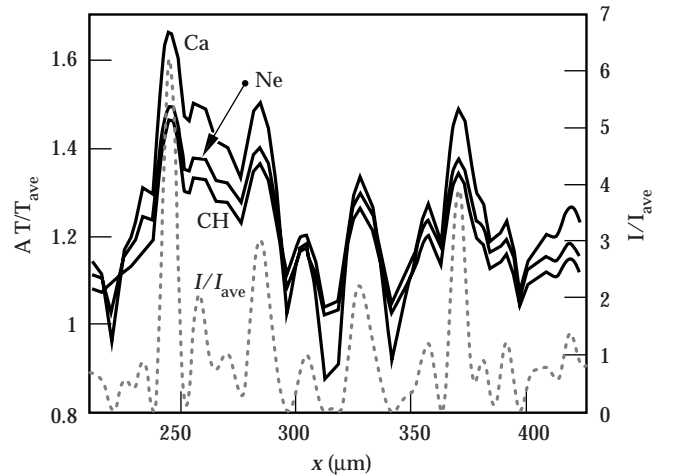


FIGURE 3. The ratio of the sound speed squared using the distribution function from Fokker-Planck simulations to that of a Maxwellian plasma at the same average temperature vs lateral position  $x$  for CH, Ne, and Ca plasmas at a tenth critical density and with an average temperature of 2.26 keV. This is the  $A$  factor which boosts the IAW temperature with respect to the energy temperature, multiplied by the spatially varying temperature normalized to the average temperature:  $A T_e(x) / T_{ave}$ . Typically, 20% or more RMS spatial variation in sound speed can be attained due to this kinetic effect. (50-00-0698-1410pb01)

crossed beam gains were found with seemingly random peaks in the frequency-tuning curves in the strongly damped IAW limit. Details of the interplay between this kinetic effect and that of velocity fluctuations, which conspire to detune the instability, will be given elsewhere.<sup>17</sup> Because the two effects are complementary, this kinetic frequency shift reduces the size of velocity fluctuations required to produce an order of magnitude lower SRS gain than in a uniform plasma illuminated by a uniform laser beam to around 10%.

## The Effects of Modified Distribution Functions on EPWs and SRS

To show the effects of EPW damping reduction on parametric instabilities (PIs) driven by RPP laser beams, we solved the kinetic dispersion relation of SRS<sup>18</sup> using the FP-generated VDFs. The results are shown in Figure 4 where we plot the ratio of SRS spatial gain rate  $\kappa_{FP}$ , using VDFs obtained via FP simulations, to those of a Maxwellian at the same temperature  $\kappa_{Maxwell}$  for the Ca and Ne plasma cases. Note that more than an order-of-magnitude increase in

SRS gain rates is obtained inside hot spots even with nonlocal heat transport, which tends to smooth out the differences between the high-energy portions of the  $e^-$  VDFs at different positions. In any case, the  $e^-$  VDFs remain highly non-Maxwellian. These large gain-enhancement factors allow the occurrence of SRS at low densities and at high temperatures, which could simply not occur in a Maxwellian plasma. Elsewhere, non-Maxwellian VDFs will turn otherwise convective SRS into absolute instabilities, which would require nonlinear mechanisms to reach saturation.

## Conclusion

We have shown in this article that an order-of-magnitude or more increase in SRS gain rates may be expected from low-density and high-temperature plasmas whenever high-intensity RPP beams nonuniformly heat a plasma. This suggests that Raman can grow at densities lower than expected and at temperatures higher than expected by relying on Maxwellian assumptions. We have also noted that parametric instabilities that rely on the properties of IAWs, such as SBS, LDI and EDI, will be significantly detuned in the strong IAW damping limit because IAW frequencies were shown to be spatially modulated by 20% or more over length scales that are short compared to the interaction lengths required for significant gain.<sup>17</sup> It follows that in the presence of non-Maxwellian VDFs SRS and SBS will be highly collimated and their reflectivities naturally anti-correlated for two reasons. First, the reduction of EPW damping increases SRS gain while simultaneously detuning SBS in the strong IAW damping limit and second, in that same limit, LDI and EDI gains are reduced to the same extent as SBS. But since the former are meant to saturate SRS, their inefficiency leads to additional unhindered SRS growth. We plan to report on extensions of this work next by using filamentation-generated intensity profiles<sup>19</sup> and not just RPP ones. We have seen that in the former case, the axial extent of hot spots will be so shortened that dephasing will be substantial even for backscattering instabilities. This suggests that filamentation could potentially suppress SRS backscatter (SBBS) especially in the strong IAW damping limit, making SBBS more likely at lower densities (where hot-spot lengths would be long) than at higher densities where filamentation would be rampant and the correlation lengths of hot spots would be much shorter, making the concomitant modulations of the frequency of IAWs ever more effective in suppressing SBBS and LDI.

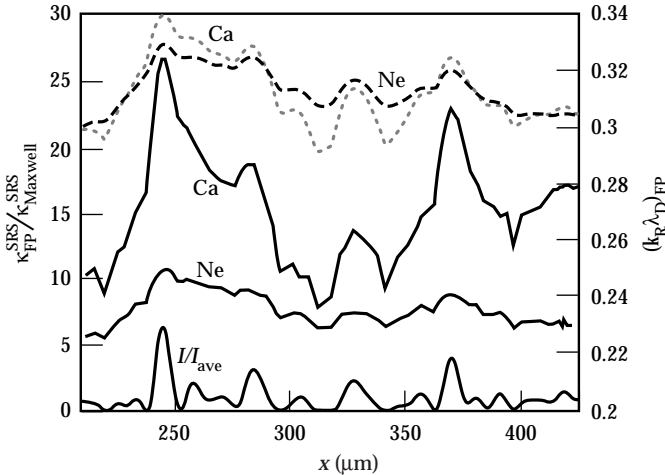


FIGURE 4. The spatial gain coefficient for stimulated Raman backscattering, using the distribution functions generated by Fokker-Planck simulations, normalized to that of a Maxwellian plasma at the same temperature vs lateral position  $x$  for Ca ( $\bar{Z} = 20$ ), and Ne ( $\bar{Z} = 10$ ), plasmas at a tenth critical density and with an average temperature of 2.26 keV. Also plotted are the real frequencies of the most unstable modes (dotted and dashed curves) and the intensity profile of the RPP beam. Order-of-magnitude increases in gain rates over Maxwellian plasmas are obtained. (50-00-0698-1411pb01)

## Acknowledgments

We gratefully acknowledge discussions with D. Montgomery, J. Fernandez, J. Moody, S. Glenzer, R. Kirkwood, T. Johnston, and V. Tikhonchuk. The work of R. P. J. Town was supported by the U. S. Department of Energy Office of Inertial Confinement Fusion under Cooperative Agreement No. DE-FC03-92SF19460 and the University of Rochester.

## Notes and References

1. A. R. Bell et al., *Phys. Rev. Lett.* **46**, 243, (1981); P. Mora and H. Yahi, *Phys. Rev. A* **26**, 2259 (1982); J. A. Albritton, *Phys. Rev. Lett.* **50**, 2078 (1983) and **57**, 1887 (1986).
2. A. B. Langdon, *Phys. Rev. Lett.* **44**, 575 (1980); R. D. Jones, and K. Lee, *Phys. Fluids* **25**, 2307 (1982); P. Alaterre, J.-P. Matte, and M. Lamoureux, *Phys. Rev. A* **34**, 1578 (1986); J. M. Liu et al., *Phys. Plasmas* **1**, 3570 (1994).
3. J. P. Matte et al., *Plasma Phys. Cont. Fusion* **30**, 1665 (1988).
4. K. Nishikawa and C. S. Liu, *Advances in Plasma Physics*, Vol. 16, (A. Simon and W. Thompson, eds.) p. 3-81, 1976.
5. B. B. Afeyan, A. E. Chou, and W. L. Kruer, *Effects of Non-Maxwellian Velocity Distribution Functions on Parametric Instabilities*, *ICF Quarterly Report* 7(2), 78, Lawrence Livermore National Laboratory, Livermore, CA, UCRL-LR-105821-97-2 (1997), and to be submitted to *Phys. Rev. E*.
6. W. L. Kruer, *The Physics of Laser Plasma Interactions*, Frontiers in Physics series, number 73. (Addison-Wesley Publishing Company, 1988).
7. D. S. Montgomery et al., *Phys. Plasmas* **3**, 1728, (1996).
8. Such as stimulated Brillouin scattering (SBS), which involves light scattering off IAWs; the Langmuir decay instability, which involves an EPW decaying into another EPW and an IAW; and the electromagnetic decay instability, which involves an EPW decaying into an electromagnetic wave and an IAW.
9. D. S. Montgomery et al., *Phys. Plasmas* **5**, 1973 (1998).
10. R. K. Kirkwood et al., *Phys. Rev. Lett.* **77**, 2706, (1996); J.C. Fernandez et al., *ibid* 2702.
11. R. K. Kirkwood et al., *Phys. Rev. Lett.* **76**, 2065, (1996).
12. Y. Kato et al., *Phys. Rev. Lett.* **5**, 1057 (1984).
13. S. M. Dixit et al., *Appl. Optics* **32**, 2543 (1993).
14. E. M. Epperlein, *Lasers and Particle Beams* **12**, 257, (1994).
15. C. T. Dum, *Phys. Fluids* **21**, 945 and 956 (1978).
16. C. Rousseaux et al., *Phys. Fluids* **B5**, 920 (1993) ; V. Yu. Bychenkov, W. Rozmus, and V. T. Tikhonchuk, *Phys. Plasmas* **4**, 1481 (1997); J. Zheng, C. X. Yu, and Z. J. Zheng, *Phys. Plasmas* **4**, 2736 (1997).
17. B. B. Afeyan et al., "Effects of Fluctuations in Ambient Flow and in the Laser Intensity on the Stimulated Brillouin Scattering Instability," *Bull. Amer. Phys. Soc.*, 7R.08, Nov. 1995 and manuscript in preparation.
18. J. F. Drake et al., *Phys. Fluids* **17**, 778 (1974).
19. A. J. Schmitt and B. B. Afeyan, *Phys. Plasmas*, **5**, 503, 1998.